PERGAMON

Available online at www.sciencedirect.com

SCIENCE DIRECT®

Electrochimica Acta 48 (2003) 4301–4309

ELECTROCHIMICA Acta

www.elsevier.com/locate/electacta

# Cr(III) oxidation with lead dioxide-based anodes

D. Devilliers [a,*,1], M.T. Dinh Thi [a,b], E. Mahé [a], Q. Le Xuan [b]

[a] *LI2C Laboratory, Université Pierre & Marie Curie, CNRS UMR 7612, 4 Place Jussieu, 75252 Paris Cedex 05, France*
[b] *Institut de Technologie Tropicale, CNST, VN, 18, Route Hoang Quoc Viet, Hanoi, Viet Nam*

Received 15 July 2003; received in revised form 29 July 2003; accepted 29 July 2003

## Abstract

A procedure for preparing $PbO_2$-based electrodes with a titanium substrate is proposed. A platinum underlayer is first deposited on Ti by metal organic chemical vapor deposition (MOCVD), followed by the electrodeposition of the $PbO_2$ layer. The prepared Ti/Pt/$PbO_2$ anodes were examined by scanning electron microscopy (SEM) and X-ray diffraction (XRD) before being used for oxidation of Cr(III) in sulphuric acid. The current efficiency was determined for that electrodes and the results were compared with those obtained with Pb/$PbO_2$ and Ebonex®/$PbO_2$ electrodes with different pH conditions. The Ti/Pt/$PbO_2$ were found to have a very good electrochemical behaviour (current efficiency: $\phi = 0.93$ for pH 2), and may be used as dimensionally stable anodes for the oxidation of Cr(III).

*Keywords:* Lead dioxide electrode; Titanium-based electrode; Chromate; Electrodeposition

## 1. Introduction

Soluble Cr(VI) species are useful in many sectors of industry [1]. For example, Cr(VI) is a redox mediator in the preparation of anthraquinone from anthracene, but it is also used for electropolishing or pickling (metal finishing). The waste baths often contain sulphuric acid, in the concentration range 0.005–3 $\text{mol}\,\text{l}^{-1}$ [1]. Their disposal is problematical for environment and the discharge of Cr species in effluents must be minimised. Hence, it is preferable to regenerate Cr(VI) from those solutions by electrolysis treatment [2].

Cr(III) oxidation has already been studied during the last 30 years; work in the field has been the object of review articles [3,4]. The anodic material used for the oxidation of Cr(III) into Cr(VI) species is often lead dioxide, which can be electrodeposited on different substrates. The preparation and properties of such anodes have been reviewed [5,6]. $PbO_2$ may be described as a non-stoichiometric compound with changing stoichiometry [6]. The main interests of $PbO_2$ anodes are: low price compared to noble metals, chemical stability in corrosive media, and high value of the overpotential for the oxygen evolution reaction [6].

The electrodeposition of $PbO_2$ has been studied on a variety of substrates: platinum [7–10], gold [11–13], graphite, glassy carbon [14], tin oxide [15], titanium [12,16,17], ceramic materials composed of Magnéli phase titanium oxides $Ti_4O_7$ and $Ti_5O_9$ called Ebonex® [18,19], stainless steel [17], and lead or a lead alloy [1].

Lead substrates usually have poor performances. The electrochemical deposition of $PbO_2$ on Ebonex® substrates leads to good adherence coatings, but it is difficult to obtain cheap large electrodes. Precious metals are too expensive. Although graphite substrates are still in use in the industry, titanium-based electrodes must be considered because they could constitute “dimensionally stable anodes” and allow thinner and mechanically superior cell designs. However, it is difficult to prepare adherent $PbO_2$ coatings on titanium. It is the reason why it is often necessary to deposit an intermediate layer between the Ti substrate and the electroactive $PbO_2$. In addition, it is necessary to avoid corrosion and passivation of titanium if the electrodes are to be used as anodes in acidic media. Pre-treatment of the substrate is very important for avoiding the formation of a $TiO_2$ passive layer. The intermediate phase must be non porous and conductive.

Conducting undercoatings which inhibit titanium oxide formation (carbides or borides of Ta or Ti) have been proposed [20]. Other authors recommend the deposition of a metal, for example a 10 μm thick tin layer [17]. Ueda

---

[*] Corresponding author. Tel.: +33-1-44-27-36-77; fax: +33-1-44-27-38-56.
*E-mail address:* devill@ccr.jussieu.fr (D. Devilliers).
[1] ISE member.

0013-4686/$ – see front matter © 2003 Elsevier Ltd. All rights reserved.
doi:10.1016/j.electacta.2003.07.005

et al. [16] have proposed a conductive undercoating consisting of Ti–Ta oxides prepared by several applications of decomposable compounds of Ti and Ta [16] followed by heat-treatment. Its conductivity is enhanced by several applications of a solution containing a thermally decomposable compound of platinum followed by subsequent heat treatments.

Electrochemical deposition of $PbO_2$ often occurs in acidic medium. In that conditions, tetragonal $\beta$-$PbO_2$ is preferably formed, so that the term "$PbO_2$" used in applied electrochemistry usually refers to the $\beta$-form [16]. However, the coating prepared in acidic medium is not sufficiently adherent to the Ti substrate, except if additives such as sodium lauryl sulphate are added to the electrolyte [21]. The second common variety of lead dioxide, i.e. orthorhombic $\alpha$-$PbO_2$, can be deposited from an alkaline solution (for example, sodium acetate, lead acetate and KOH). Too alkaline solutions give rise to the formation of red $Pb_3O_4$ crystals on the electrodes [22]. $\alpha$-$PbO_2$ has a more compact structure compared to the more porous $\beta$-$PbO_2$ [23], resulting in a better contact between the particles.

When the procedure gives rise to a mixture of the two crystallographic varieties, the quantitative determination of each phase is not easy but one can compare, in the X-ray diffractograms obtained with different samples, the ratio of the peak areas $\alpha/(\alpha+\beta)$ and $\beta/(\alpha+\beta)$ [23]. Other authors [10,24] use the procedure of Dodson [25], based on calibration spectra obtained with pure $\alpha$ and $\beta$ varieties. However, the results cannot be very accurate since electrodeposited $PbO_2$ is always textured and the preferred crystallographic orientations that are observed depend on several parameters: temperature, potential, current density. Nevertheless, in $Pb(NO_3)_2$–$HNO_3$ electroplating solutions, the amount of $\alpha$-phase decreases with temperature and, at 65 °C, only the $\beta$-phase was detected on a Pt substrate [10], with a preferential orientation of the planes: (1 1 1). An increase of temperature is reported to favour the formation of larger crystals [10].

In order to increase the electrocatalytic activity of $PbO_2$ towards various anodic reactions, incorporation of some ions into the oxide layer film during its formation was examined in the literature [23,26].

Ueda et al. [16] have proposed a galvanostatic procedure in which a stress-free intermediate $\alpha$-$PbO_2$ coating is produced by electrodeposition from an alkaline lead bath. It plays the role of binder on the top of which $\beta$-$PbO_2$ can be electrodeposited from an acid lead bath containing a suspension of fine $Ta_2O_5$ particles. These particles are incorporated into the $\beta$-$PbO_2$ layer in order to result in a coating with low internal stress. That procedure led to an anode material which is reported to be superior to $Pb/PbO_2$ or Ti/Pt with respect to oxygen overvoltage [16]. However, the preparation mode is long, especially the formation of the undercoating; in addition, its conductivity is enhanced by a platinum deposit but its compactness is probably not sufficient for avoiding completely the corrosion of the Ti substrate that may occur in acidic media.

In this paper, we report a simplified procedure for preparing a $Ti/Pt/PbO_2$ electrode, in which the underlayer in contact with Ti and $PbO_2$ is a compact film of platinum, deposited by metal organic chemical vapor deposition (MOCVD). The prepared anodes were used for oxidation of Cr(III) in sulphuric acid. The results were compared with those obtained with $Pb/PbO_2$ and Ebonex®/$PbO_2$ electrodes. These experiments were realised in a two-compartment cell containing an anionic membrane as a separator the current yield was determined for the three electrode substrates with different pH conditions.

## 2. Experimental

### 2.1. Preparation of the working electrodes

All chemicals were Prolabo Normapur grade, except when specified hereafter. Titanium foils (Goodfellow; purity: 99.6%; area: 4 $cm^2$) were carefully polished on abrasive papers Buehler-Met 600, 800 and 1200, and rinsed with methanol in an ultrasonic cleaner.

First, a thin and compact platinum film was deposited on one face of the foil by MOCVD. This method is based on the oxidative decomposition of (methylcyclopentadienyl) trimethyl platinum(IV) (Strem; purity 99%) as a precursor, diluted in cyclohexane solvent [27]. A Trijet liquid delivery system has been used to supply and vaporize the precursor solution ($C = 0.02$ M) into the reactor. Helium carrier gas and oxygen reactant gas were used at a pressure of 1330 Pa. The other experimental conditions for the deposition of platinum films were: temperature of the evaporator: 48 °C; platinum deposition temperature $\Theta = 350\,^{\circ}C$; deposition time: $\tau = 4000$ s. With such conditions, the thickness of the film is about 16 nm and platinum oxide is not formed: ESCA experiments have proved that the atomic percentage of oxygen is less than 0.1% with those experimental conditions of deposition [27]. That platinum layer was prepared for avoiding passivation or corrosion of the Ti substrate during all the subsequent experiments. Thus, the back side of the foils was insulated by application of an epoxy resin.

Second, an undercoating of $\alpha$-$PbO_2$ was electrodeposited from an alkaline lead bath (called S1 hereafter), as reported by other authors [16]: 3.5 M NaOH saturated with litharge PbO (pure; Touzart & Matignon) at $\Theta = 40\,^{\circ}C$. The pH of S1 is >14 and the soluble Pb(II) species are $HPbO_2^-$ anions. The cyclic voltammogram performed at $v = 50\,mV\,s^{-1}$ is presented in Fig. 1a. It shows that the $PbO_2$ deposition begins at potentials higher than 0.25 V/ECS. Thus, for our potentiostatic experiments, a constant potential (0.35 V versus SCE) was applied for 2 h. Those potentiostatic conditions led to homogeneous lead dioxide deposits.

Thus, the top coating ($\beta$-$PbO_2$) was electrodeposited from an acid lead bath [5], called S2, and containing 30 wt.% $Pb(NO_3)_2$ (pH 2). That bath, kept at $\Theta = 65\,^{\circ}C$, was

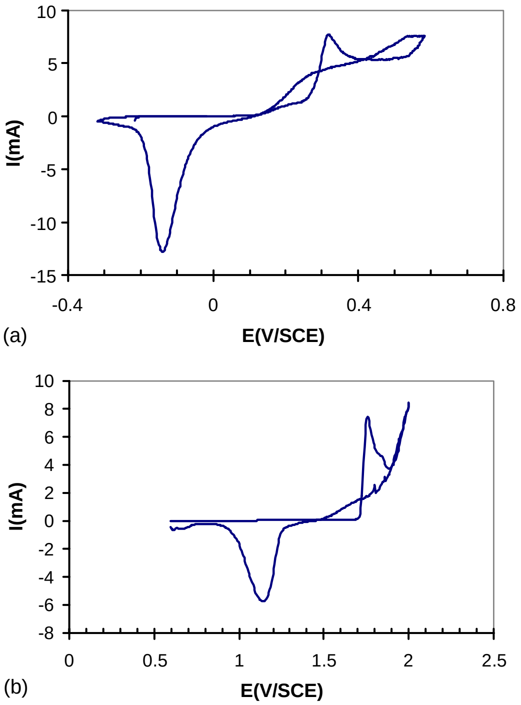

Fig. 1. (a) Cyclic voltammogram performed at $v = 50\,\mathrm{mV\,s^{-1}}$ with the alkaline solution S1. Working electrode: Ti/Pt; $S = 4\,\mathrm{cm^2}$, (b) cyclic voltammogram performed at $v = 50\,\mathrm{mV\,s^{-1}}$ with the acid solution S2. Working electrode: Ti/Pt; $S = 4\,\mathrm{cm^2}$.

continuously agitated and was containing a suspension of $Ta_2O_5$ powder (5 g/l; Aldrich; purity: 99%) in order to prepare a coating with low internal stress. The cyclic voltammogram performed at $v = 50\,\mathrm{mV\,s^{-1}}$ is presented in Fig. 1b. It shows that the $PbO_2$ deposition begins at potentials higher than 1.7 V/SCE. Thus, for our potentiostatic experiments, a constant potential (1.8 V versus SCE) was applied for 3 h. For such temperatures of the electroplating solution (65 °C), the lifetime of the electrodes is reported to be higher than that of samples obtained at room temperature [10].

The loading of the undercoating ($\alpha$-$PbO_2$) and top coating ($\beta$-$PbO_2$) was estimated to be 31 and 13 μm, respectively. These results were obtained by the following technique: after the $PbO_2$ layer was formed, the electrode was immersed in hot concentrated nitric acid (8 M); the dissolution of $PbO_2$ occurred and led to soluble Pb(II). Its concentration was determined by square wave voltammetry, using a mercury electrode. Thus, the thickness of the $PbO_2$ layers was evaluated, knowing its density ($\rho = 9.375\,\mathrm{g\,cm^{-3}}$).

The loading of $Ta_2O_5$ mechanically incorporated into the $PbO_2$ layer is not known. Other authors using the same procedure do not give that information [16].

The lead foils were provided by Weber Métaux, Paris, and the Ebonex® ceramics (non porous grade) by Atraverda Ltd. For the Ebonex® substrate, no platinum film was necessary; the $PbO_2$ film was directly deposited according to the procedure reported above. On the lead substrate, no $PbO_2$ layer was electrodeposited from the S1 or S2 solutions, because it is well-known that such a layer is formed when lead electrodes are used as anodes.

The $PbO_2$ layers were characterized by scanning electron microscopy (SEM, Leica Stereoscan 440). In addition, X-ray diffraction (XRD) spectra were obtained with a Philips 1380 diffractometer. The X-ray tube was operated at 30 kV with a molybdenum target. The wavelength of the K$\alpha$1 emission line is: $\lambda = 0.70930$ Å.

### 2.2. *Electrolysis of Cr(III) solutions*

The oxidation of Cr(III) was carried out in a two-compartment cell, under galvanostatic conditions ($j = 10\,\mathrm{mA\,cm^{-2}}$), at 25 °C during 24 h, using an EG&G 273A potentiostat/galvanostat. The anodic compartment (V = 0.2 L) was containing the $PbO_2$ working electrode dipped in a 0.1 M Cr(III) solution acidified by $H_2SO_4$ at several concentrations (0.5, 0.05 or 0.005 M). Cr(III) was introduced as $KCr(SO_4)_2$ Merck pro analysi. Before the macro-electrolysis started, the limiting current density for Cr(III) oxidation was determined, taking into account the mass transfer conditions in the anodic compartment (continuous stirring at constant speed). Its value was: $j_L = 25\,\mathrm{mA\,cm^{-2}}$. The charge was calculated so that less than 60% of the initial Cr(III) species could be oxidized.

The cathodic compartment was containing a graphite counter-electrode dipped in sulphuric acid.

For the study of the overall current efficiency, the Cr(VI) concentration was determined at the end of the 24 h experiment. An anion-permeable membrane Asahi Chemical A10 was used as a separator.

The determination of Cr(VI) concentrations can be made by titration with Mohr's salt, with phenylanthranilic acid as indicator [28]. It is also possible to plot the reduction wave of Cr(VI) and to measure the limiting diffusion current intensity, $i_{\mathrm{Lred}}$, obtained with a rotating disk electrode (RDE). However, platinum electrodes are not recommended because acidic Cr(VI) solutions attack the metal, and the oxide film formed hinders the electrode reaction. On the contrary, gold electrodes are suitable [29]. Thus, we have chosen to determine the Cr(VI) concentration in the anodic compartment with a Tacussel RDE fitted with a gold disk (diameter: 2 mm) and operated at a 3000 rpm rotation speed. All the experiments were performed after 10 min argon bubbling for removing dissolved oxygen. A small amount of anolyte (1 cm$^3$) was removed and diluted in 40 cm$^3$ of 0.5 M sulphuric acid. The value of the limiting current intensity due to the reduction of Cr(VI), $i_L$, was determined and the concentration of Cr(VI) was deduced from the calibration curve $i_L = f(C)$. That curve was plotted previously, using $2.5 \times 10^{-4} - 2 \times 10^{-3}$ M standard solutions of Cr(VI) in 0.5 M sulphuric acid.

The instantaneous current efficiency was also determined in a shorter time range (12.5 h). For that experiments, the two-compartment cell was used, fitted with an anionic membrane Ionac MA-3475. The anolyte was composed of $KCr(SO_4)_2$ 0.1 M + $H_2SO_4$ (0.05 M) and the catholyte was $H_2SO_4$ 0.05 M. 15 ml of anolyte were periodically removed from the electrolysis cell and transferred into another cell fitted with a rotating gold electrode, an SCE reference electrode and a platinum counter electrode. After the measurement of the concentration of Cr(VI) from the limiting reduction current intensity, the 15 ml of solution were reintroduced into the electrolysis cell.

## 3. Results and discussion

### 3.1. Structural analysis and morphology of the $PbO_2$ deposits

The aim of these investigations was first to verify the nature of the $PbO_2$ deposits ($\alpha$ or $\beta$ variety) and also to determine the size of the crystallites.

The titanium substrate covered by the platinum film deposited by MOCVD was first studied by SEM. The micrography presented in Fig. 2 shows the morphology of the surface. The stripes resulting from the mechanical polishing of the titanium substrate are clearly visible, but it is not necessary to have a perfectly flat substrate for depositing adherent $PbO_2$ on it. The thickness of the Pt deposit was estimated by energy dispersion spectrometry. Its value (about 20 nm) is in agreement with the expected one (16 nm, see Section 2).

Electrodeposition of a $PbO_2$ coating on a Ti/Pt substrate from an alkaline solution (S1) was performed under the potentiostatic conditions described above. The corresponding sample, called “Sample 1” hereafter, was observed by SEM. It seems very compact (see Fig. 3). The pyramidal form of the $\alpha$-$PbO_2$ crystallites cannot be easily distinguished. Their size is about 1 μm. The same morphology was observed for a $PbO_2$ deposit on Ebonex®.

After, another sample, called “Sample 2” was prepared by electrodeposition of $PbO_2$ on a Ti/Pt substate from the acid S2 solution. The resulting deposit is compact. Two kinds of crystallites can be distinguished on the surface: small $\beta$-$PbO_2$ crystals (size $< 0.5\,\mu m$) and also large pyramidal-form $\alpha$-$PbO_2$ crystals (size: 3 μm), as shown in Fig. 4. The $\alpha$-$PbO_2$ crystals formed in the S2 solution are about three times larger than those formed in the S1 solution.

On several places of the surface, $Ta_2O_5$ particles are embedded into the $PbO_2$ layer. Such a particle is visible in Fig. 5; its size is about 7 μm.

Other authors claim that the $\alpha$ variety was obtained using the S1 solution, and the $\beta$ variety using the S2 solution [16]. However, they did not give any structural analysis data, and their procedure was different: they performed galvanostatic electrodeposition, whereas we worked under potentiostatic conditions.

In order to confirm the presence of the two varieties of $PbO_2$ on the electrodes, XRD experiments were performed with Samples 1 and 2. The corresponding X-ray spectra are presented in Figs. 6 and 7, respectively.

The important background is due to the absorption of the radiation by the sample containing lead, and emission of the absorbed energy as fluorescent radiation in all directions.

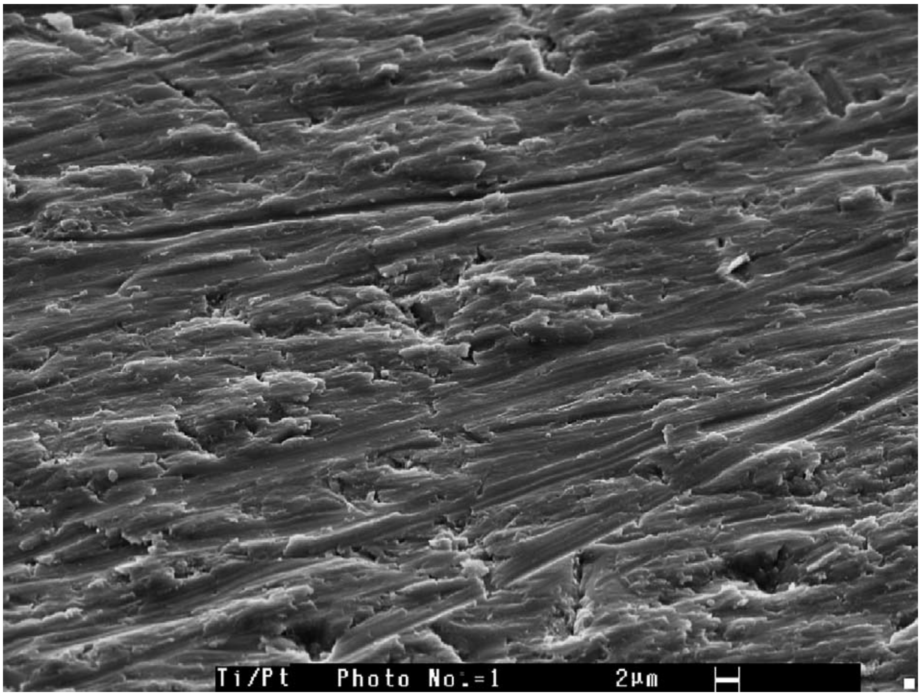

Fig. 2. Platinum deposit on a titanium substrate (bar scale = 2 μm).

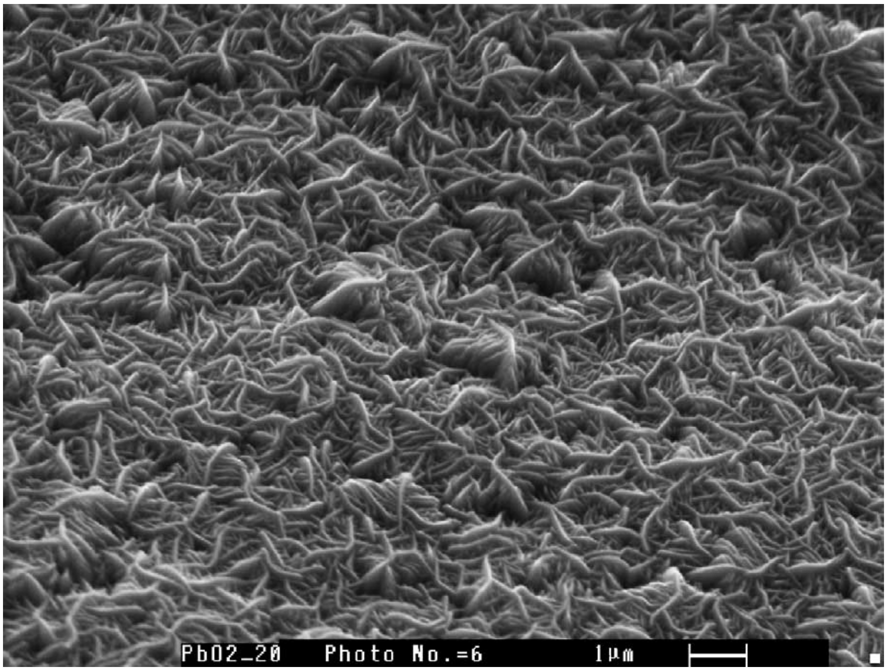

Fig. 3. $PbO_2$ electrodeposited on Ti/Pt from the alkaline solution S1 (bar scale = 1 µm).

Attribution of the peaks was performed by using JCPDS data. The results are reported in Tables 1 and 2. It can be concluded that Sample 1 is mainly composed of $\alpha$-$PbO_2$, but all the characteristic peaks of $\alpha$-$PbO_2$ variety are not visible. The (2 0 0) line has the highest intensity. $\beta$-$PbO_2$ may also be present (the peaks at $2\theta = 16.46$ and $33.28^\circ$ can be attributed to both varieties) but only very small amounts may be present, otherwise other characteristics peaks of the $\beta$-variety should be observed. The peak at $26.79^\circ$ may be attributed only to the $\alpha$ variety.

On the contrary, for Sample 2, the $\beta$-$PbO_2$ variety is mainly present, and the preferred orientations planes are (0 1 1) and (1 0 1). The $\alpha$-variety is also clearly identified, especially from the peak at $2\theta = 13.08^\circ$ corresponding to the (1 1 1) plane.

Our results differ to a certain extent from other results published in the literature. The amount of $\alpha$-$PbO_2$ in Sample 2, prepared at 65 °C, is less important that in other $PbO_2$ layers deposited on titanium from a $Pb(NO_3)_2$–$HNO_3$ solution by Devos [30,31], working at ambient temperature.

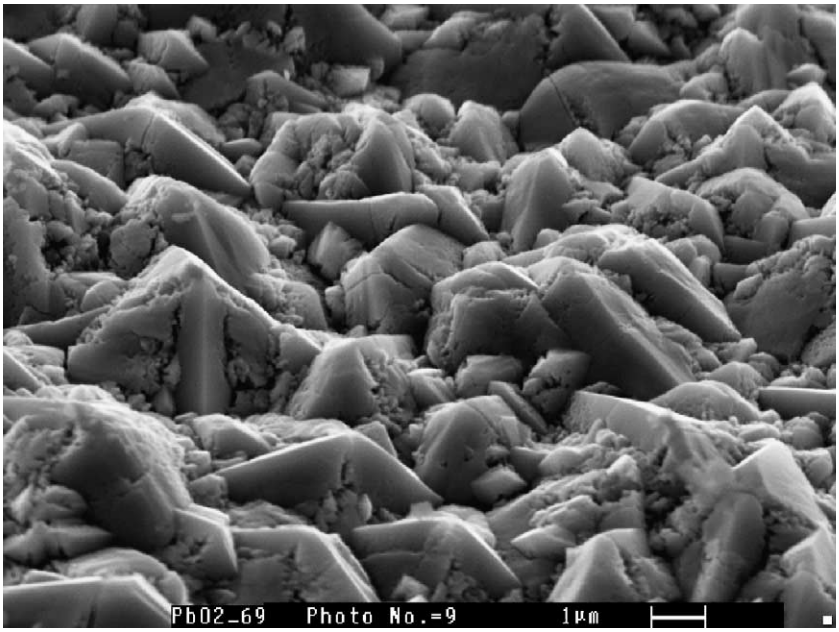

Fig. 4. $PbO_2$ electrodeposited on Ti/Pt/$PbO_2$ from the acid solution S2 (bar scale = 1 µm).

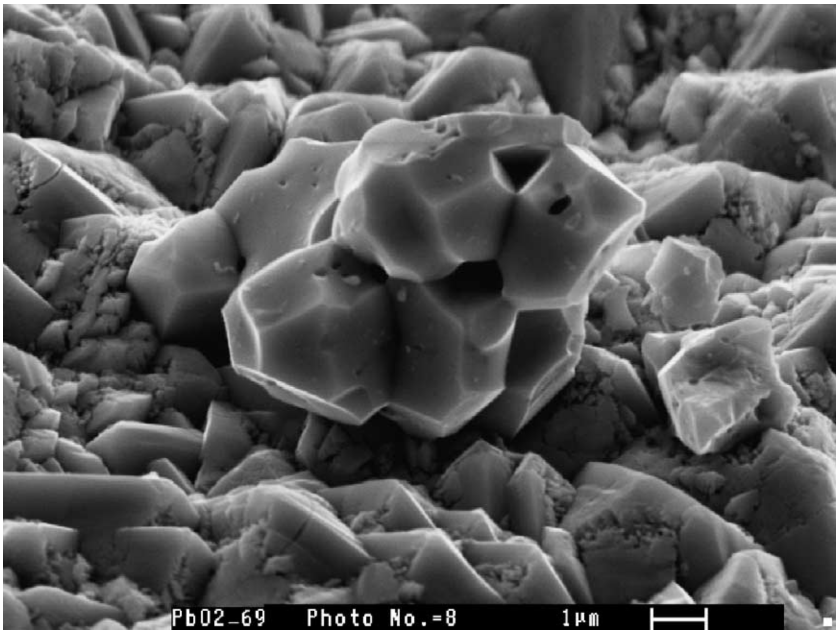

Fig. 5. $Ta_2O_5$ crystals embedded into the $PbO_2$ layer electrodeposited from the S2 solution (bar scale = 1 μm).

However, Velichenko et al. [10] did not observe the α variety in $PbO_2$ deposited at 65 °C on a platinum substrate.

### 3.2. Electrolysis of Cr(III) solutions

During electrolysis, the following reactions occur:

- at the anode:

$$2\,Cr^{3+} + 7\,H_2O \rightarrow Cr_2O_7{}^{2-} + 14\,H^+ + 6\,e^-$$

or:

$$2\,H_2O \rightarrow 4\,H^+ + O_2 + 4\,e^-$$

- at the cathode:

$$2\,H^+ + 2\,e^- \rightarrow H_2$$

The oxidation of Cr(III) competes with the oxidation of water. Thus, it was necessary to determine the current efficiency, $\phi$, of the Cr(VI) production for different experimental conditions (pH 0, 1 or 2 with the three substrates).

As described in the Section 2, the calibration curve $i_L$ = f ($Cr^{VI}$) was plotted, using standard solutions of Cr(VI) in 0.5 M sulphuric acid.

The determination of the amount of Cr(VI) formed in the electrolysis cell was performed at the end of the 24 h experiments. A small amount of anolyte was removed from the cell and diluted in 0.5 M sulphuric acid. In such conditions, both standard solutions and solutions with unknown Cr(VI) concentration had similar pH value and ionic strength.

The values of the overall current efficiency, $\phi$, for 24 h electrolysis at $j = 10\,mA\,cm^{-2}$ are reported in Table 3.

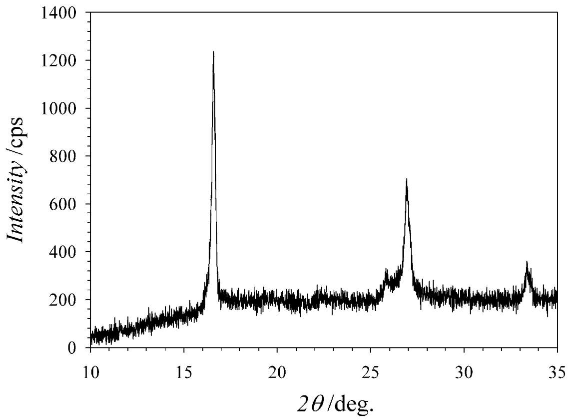

Fig. 6. XRD spectrum obtained with Sample 1 ($PbO_2$ electrodeposited from the alkaline solution S1).

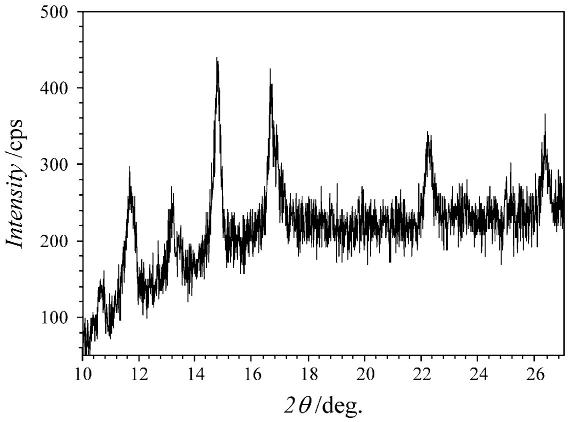

Fig. 7. XRD spectrum obtained with Sample 2 ($PbO_2$ electrodeposited from the acid solution S2).

Table 1
XRD data for $PbO_2$ electrodeposited with the alkaline S1 solution (Sample 1)

| Experimental diffraction angles $2\theta$ (°) | Relative intensity | $PbO_2$ variety | Diffraction angles $2\theta$ (°) for $\alpha$-$PbO_2$ and $(h\,k\,l)$ indexation JCPDS data | Relative intensity | Diffraction angles $2\theta$ (°) for $\beta$-$PbO_2$ and $(h\,k\,l)$ indexation JCPDS data | Relative intensity |
|---|---|---|---|---|---|---|
| 16.46 | 100 | α or β | (2 0 0) at 16.44° | 20 | (020) at 16.44° | 30 |
| 26.79 | 46 | α | (3 1 1) at 26.80° | 30 | – | – |
| 33.28 | 15 | α or β | (4 0 0) at 33.24° | 30 | (040) at 33.24° | 5 |

The values of diffraction angles for α and β-$PbO_2$ are extracted from the literature.

Table 2
XRD data for $PbO_2$ electrodeposited with the acid S2 solution (Sample 2)

| Experimental diffraction angles $2\theta$ (°) | Relative intensity | $PbO_2$ variety | Diffraction angles $2\theta$ (°) for $\alpha$-$PbO_2$ and $(h\,k\,l)$ indexation JCPDS data | Relative intensity | Diffraction angles $2\theta$ (°) for $\beta$-$PbO_2$ and $(h\,k\,l)$ indexation JCPDS data | Relative intensity |
|---|---|---|---|---|---|---|
| 10.57 | 24 | α | (1 1 0) at 10.63° | 12 | – | – |
| 11.61 | 70 | β | – | – | (1 0 1) at 11.60° | 100 |
| 13.08 | 46 | α | (1 1 1) at 13.05° | 100 | – | – |
| 14.69 | 100 | β | – | – | (0 1 1) at 14.55° | 95 |
| 16.59 | 84 | α or β | (2 0 0) at 16.44° | 20 | (0 2 0) at 16.44° | 30 |
| 22.14 | 47 | α or β | (1 3 0) at 22.23° | 45 | (1 2 1) at 22.04° | 70 |
| 26.22 | 50 | α or β | (2 2 2) at 26.28° | 17 | (1 3 0) at 26.11° | 16 |

The values of diffraction angles for α- and β-$PbO_2$ are extracted from the literature.

With the three substrates, $\phi$ increases with the pH value. That result is in agreement with those obtained by Kuhn and Clarke [29]. Higher values of $\phi$ are expected for higher values of pH because protons are formed during the formation of $Cr_2O_7^{2-}$.

The highest $\phi$ values were obtained for $[H_2SO_4] = 0.005$ M (ca. pH 2) for all the substrates, but the best results were obtained with Ti/Pt/$PbO_2$ ($\phi = 0.93$). Higher pH values were not tested, because they correspond to unrealistic industrial solutions.

It is shown from Table 3 that the Ti/Pt/$PbO_2$ electrodes exhibit the best performances. Ebonex®/$PbO_2$ electrodes also give interesting results but it must be kept in mind that even the “Non porous grade” Ebonex® substrates have a residual porosity that allows the electrolyte to diffuse up to the electric contact, leading to its corrosion [32].

At last, lead anodes on which the $PbO_2$ is formed in situ during the electrochemical oxidation of Cr(III) do not exhibit good results.

After the 24 h experiments, the Ti/Pt/$PbO_2$ electrodes were examined again by SEM. The $PbO_2$ layer deposited on Ti remained still compact and adherent to the surface.

Table 3
Overall current efficiency for the oxidation of 0.1 M Cr(III) on three kinds of $PbO_2$ electrodes at several sulphuric acid concentrations after 24 h electrolysis at $j = 10\ \mathrm{mA\,cm^{-2}}$

| $[H_2SO_4]$/M | 0.5 | 0.05 | 0.005 |
|---|---|---|---|
| Ti/Pt/$PbO_2$ | 0.60 | 0.80 | 0.93 |
| Ebonex®/$PbO_2$ | 0.55 | 0.57 | 0.74 |
| Pb/$PbO_2$ | 0.21 | 0.44 | 0.56 |

The instantaneous current efficiency was determined for a 12.5 h electrolysis at $j = 10\ \mathrm{mA\,cm^{-2}}$, performed with the Ti/Pt/$PbO_2$ electrode as described above (Section 2). As it can be seen from Fig. 8, ϕ decreases slightly with time from 0.985–0.885, but its value remains very high. The total voltage of the cell, $\Delta U$, was monitored continuously during the experiment. Its initial value (20 V) is quite high because the ohmic drop is very important in our laboratory cell. Nevertheless, the value of $\Delta U$ continuously increased. The value at the end of the 12.5 h experiment was 29 V. That increase is attributed to the important decrease of the conductivity of the catholyte. Indeed, as shown in Fig. 9, the concentration of sulphuric acid decreases sharply in that compartment because $H^+$ cations are consumed at the cathode ($H^+$ are brought to the electrode both by migration and diffusion), whereas $SO_4^{2-}$ anions move away from the compartment by

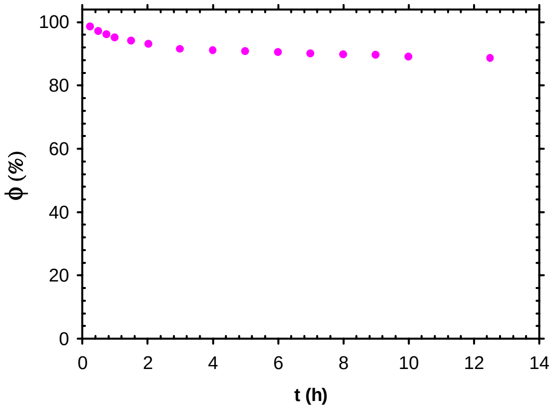

Fig. 8. Instantaneous current efficiency for the oxidation of Cr(III) on Ti/Pt/$PbO_2$ electrode at $j = 10\ \mathrm{mA\,cm^{-2}}$.

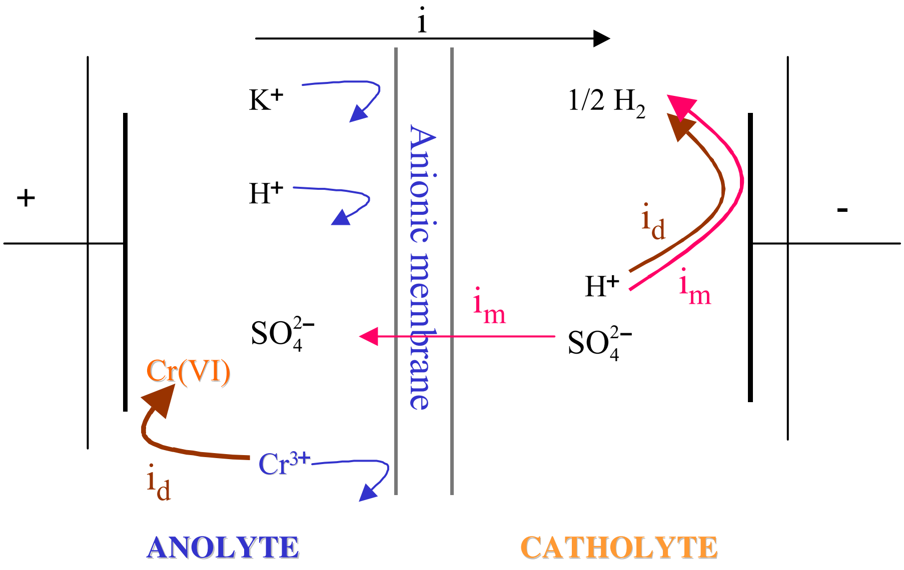

Fig. 9. Transport phenomena and electrode reactions in the electrolysis cell fitted with an anionic membrane.

migration. In Fig. 9, the contributions of diffusion and migration are indexed with “d” and “m” subscripts respectively.

## 4. Conclusion

The Ti/$PbO_2$ samples have been prepared according to the procedure reported above. The outer layer is mainly composed of β-$PbO_2$. In terms of current efficiency, these electrodes exhibit better electrochemical behaviour for the oxidation of Cr(III) species in sulphuric acid than other $PbO_2$ electrodes described in the literature. They are not as fragile as Ebonex®/$PbO_2$ electrodes and they are dimensionally stable. Long time experiments in a flow cell need now to be performed in order to determine the lifetime of these electrodes. That flow cell needs to have an optimised geometry for lowering ohmic drops.

## Acknowledgements

The SEM experiments and the X-ray diffraction spectra were performed in the Laboratoire de Physique des liquides et Electrochimie, Paris. Mr Borensztajn and Dr G. Maurin are gratefully acknowledged. The Ionac membrane was provided by Professor G. Pourcelly (UMR CNRS 5635, Montpellier). The authors express also their thanks to Drs O. Valet and P. Doppelt (ESPCI, Paris) who performed the platinum deposits and to Dr H. Groult (CNRS, Paris) for fruitful discussions.

## References

[1] D. Pletcher, F.C. Walsh, Industrial Electrochemistry, Chapman & Hall, New York 1990 (Chapters 5 and 7).
[2] A.T. Kuhn, R. Clarke, J. Appl. Chem. Biotechnol. 26 (1976) 407.
[3] K.L. Pamplin, D.C. Johnson, J. Electrochem. Soc. 143 (1996) 2119.
[4] F.I. Danilov, A.B. Velichenko, Electrochim. Acta 38 (1993) 437.
[5] J.P. Carr, N.A. Hampson, Chem. Rev. 72 (1972) 679.
[6] J.P. Pohl, H. Rickert, in: S. Trasatti (Ed.), Electrodes of Conductive Metallic Oxides, Part A, Elsevier, Amsterdam, 1980, (Chapter 4).
[7] M. Fleischmann, M. Liler, Trans. Faraday Soc. 54 (1958) 1370.
[8] B.J. Hwang, R. Santhanam, Y.W. Chang, Electroanalysis 14 (2002) 363.
[9] A.B. Velichenko, D.V. Girenko, F.I. Danilov, Russian J. Electrochem. 33 (1997) 96.
[10] A.B. Velichenko, R. Amadelli, A. Benedetti, D.V. Girenko, S.V. Kovalyov, F.I. Danilov, J. Electrochem. Soc. 149 (2002) C445.
[11] H. Chang, D.C. Johnson, J. Electrochem. Soc. 136 (1989) 17.
[12] J. Lee, H. Varda, S. Uhm, Y. Tak, Electrochem. Commun. 2 (2000) 646.
[13] A.B. Velichenko, D.V. Girenko, F.I. Danilov, J. Electroanal. Chem. 405 (1996) 127.
[14] D. Velayutham, M. Noel, Electrochim. Acta 36 (1991) 2031.
[15] C.N. Ho, B.J. Hwang, Electrochim. Acta 38 (1993) 2749.
[16] M. Ueda, A. Watanabe, T. Kameyama, Y. Matsumoto, M. Sekimoto, T. Shimamune, J. Appl. Electrochem. 25 (1995) 817.
[17] G. Cifuentes, L. Cifuentes, R. Kammel, J. Torrealba, A. Campi, Z. Metallkd. 89 (1998) 363.
[18] J.E. Graves, D. Pletcher, R.L. Clarke, F.C. Walsh, J. Appl. Electrochim. 21 (1991) 848.
[19] J.E. Graves, D. Pletcher, R.L. Clarke, F.C. Walsh, J. Appl. Electrochim. 22 (1992) 200.
[20] J. Gonzalez-Garcia, J. Iniesta, E. Exposito, V. Garcia-Garcia, V. Montiel, A. Aldaz, Thin Solid Films 352 (1999) 49.
[21] C. Bemelmans, T. O’Keefe, E. Cole, Bull. Electrochem. 12 (1996) 591.
[22] P. Rüetschi, R.T. Angstadt, B.D. Cahan, J. Electrochem. Soc. 106 (1959) 547.
[23] I. Petersson, E. Ahlberg, B. Berghult, J. Power Sources 76 (1998) 98.
[24] N. Munichandraiah, J. Appl. Electrochem. 22 (1992) 825.
[25] V.H. Dodson, J. Electrochem. Soc. 108 (1961) 401.
[26] A.B. Velichenko, D.V. Girenko, S.V. Kovalyov, A.N. Gnatenko, R. Amadelli, F.I. Danilov, J. Electroanal. Chem. 454 (1998) 203.

[27] O. Valet, P. Doppelt, P.K. Baumann, M. Schumacher, E. Balnois, F. Bonnet, H. Guillon, Microelectron. Eng. 64 (2002) 457.
[28] B.N. Laskorin, N.M. Smirnova, Y.S. Mishukova, A.V. Komarov, Zhurnal Prikladnoi Khimii (J. Appl. Chem. USSR) 47 (1974) 1870.
[29] F. Baumann, I. Shain, J. Am. Chem. Soc. 78 (1956) 5550.
[30] B. Devos, Thesis, P&M Curie University, Paris, 1997, p. 178.
[31] B. Devos, H. Groult, D. Devilliers, J.-F. Sarrau, M. Chemla, French Patent 2,788,377 (2001).
[32] J. Pouilleau, H. Groult, D. Devilliers, Journées d'Electrochimie 1995, Strasbourg, France, abstract 5–22.